RUSSIAN JOURNAL OF EARTH SCIENCES, VOL. 7, NO. 2, PAGES 1–15, APRIL 2005

The Mesozoic-Cenozoic boundary: Paleomagnetic characteristic

D. M. Pechersky

Institute of Physics of the Earth, Russian Academy of Sciences

A. V. Garbuzenko

Geological Institute, Russian Academy of Sciences

Abstract. The purpose of this paper is to consider the behavior of the geomagnetic field in the vicinity of the Mesozoic-Cenozoic (Mz-Kz) boundary, in particular, of the paleointensity and polarity of the field, the frequency of geomagnetic polarity reversals, the total magnitude of the field direction variations, and the behavior of the magnetic susceptibility of oceanic sediments in the vicinity of the Mz-Kz boundary. As to these paleomagnetic events, worthy of mention is the change in the variation conditions at the Mesozoic-Cenozoic boundary. It is global growth of the average variation magnitude from 8°–8.5° in the Late Cretaceous to 11.5° in the Early Cenozoic. The global character of this event suggests a general change in the generation of the geomagnetic field direction variations in the vicinity of the Mz-Kz boundary. A change in the Earth core conditions, causing the reversals of the geomagnetic field, began at ~80 Ma, that is, notably earlier than the Mz-Kz boundary, and, hence, was not associated directly with this boundary, nor with the generation of variations in the geomagnetic field direction. Some local changes in the variations of the magnetic field direction were associated with the formation of plumes near the core-mantle boundary, yet, the plumes have originated 20–40 million years prior to the Mz-Kz boundary. As follows from the examination of sequences of oceanic sediments (DSDP and ODP data), the Mz-Kz boundary is often, but not necessarily, marked by a peak of magnetic susceptibility (κ-peak), i.e. that is not a characteristic feature of the Mz-Kz boundary. The accumulation of magnetic materials in the sediments lasted from a few dozens of thousand years (more common estimates) to hundreds of thousand years. And, where this interval is observed, it does include the Mz-Kz biostratigraphic boundary, except for very rare cases. The Mz-Kz biostratigraphic boundary is always restricted to the C29r chron, but its position varies as a function of its paleolatitude, amounting to about 0.7 Myr. The highest κ-peak values are close to the epicenters of active plumes, but high κ-peaks have been found far from the plumes.

Paper number TJE05174.
ISSN: 1681–1208 (online)

The online version of this paper was published 24 March 2005.
URL: http://rjes.wdcb.ru/v07/tje05174/tje05174.htm

Introduction

The boundary between the Mesozoic and Cenozoic (Mz-Kz) is imprinted in significant surface and subsurface events, such as, (a) the substantial extinction of biota, (b) the intensive plume magmatic activity, expressed, in particular, in the extensive Deccan trap formation, basalt flows in Greenland (North Atlantic volcanic province), (c) the impact activity

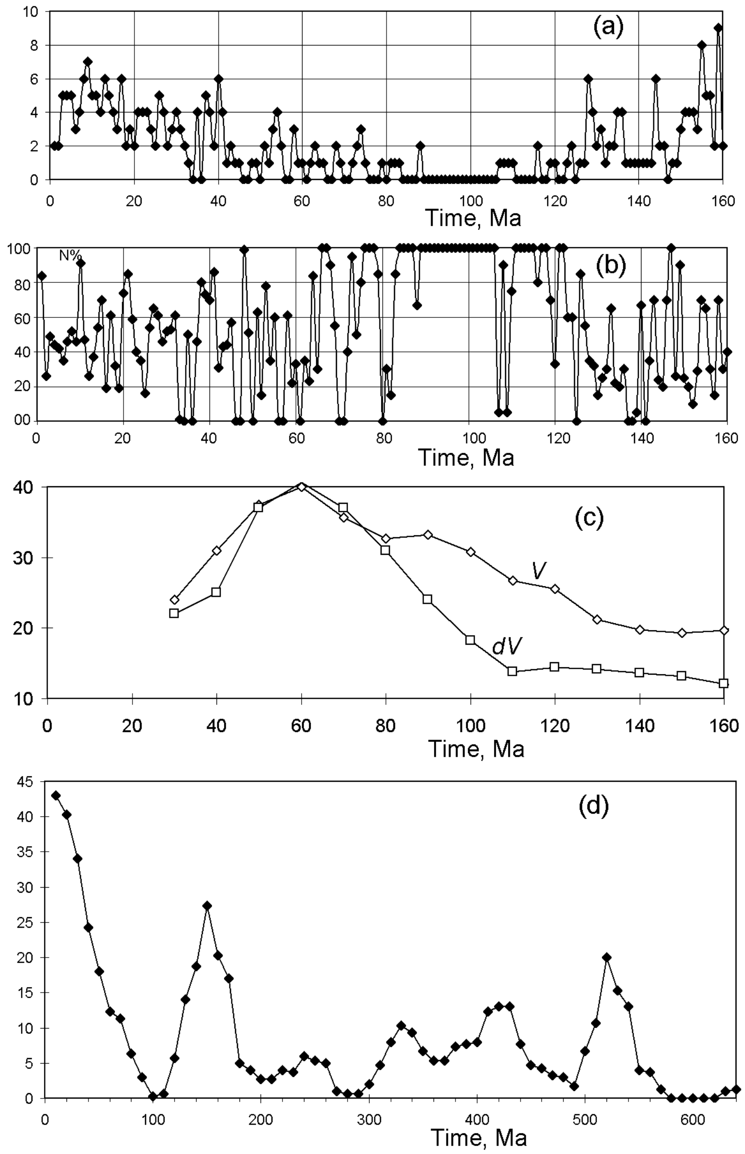

Figure 1. The behavior of the geomagnetic field and the plate movement rates for the last 160 Ma (a–c) and 640 Ma (d): (a) the number of the geomagnetic field reversals for 1 million years; (b) the contribution of direct magnetic polarity for 1 million years. The figures are plotted in the geomagnetic polarity timescale [*Cande and Kent,* 1992], specified by E. A. Molostovskii, et al. (2004); (c) the average velocity (V) of the continental plate motion and the dispersion of the plate motion rates (dV); the averaging window is 10 million years [*Jurdy et al.,* 1995; *Pechersky,* 1998]; d) the number of the geomagnetic field reversals for 10 million years [*Pechersky,* 1998].

which expressed in the anomalous contents in the sediments of cosmic-origin platinoid metals, in particular, of iridium, and in the presence of shock-metamorphosed quartz and tectites in the sediments, (d) some enrichment of oceanic and marine sediments in magnetic minerals, which is expressed in the fairly narrow anomalous peak of magnetic susceptibility at or in the vicinity of this boundary [*Alvares et al.,* 1990; *Baulus et al.,* 2000; *Courtillot et al.,* 2003; *Ellwood et al.,* 2003; *Ernst and Buchan,* 2003; *Grachev,* 2000; *Montanari et al.,* 1998; *Smith et al.,* 1982; *Veimarn et al.,* 1998], and (e) the intensification of differential plate movements which expressed in the highest dispersion of the plate movement rates against the background of the growing average velocity of the continental plate movement (Figure 1c) [*Jurdy et al.,* 1995; *Pechersky,* 1998]. The synchronism or the nearly synchronous occurrence of these events at the Earth surface obviously suggest some common mechanism responsible for them. If this mechanism involved the whole of the Earth, including its core, it must have been imprinted in the behavior of the geomagnetic field, the source of which must have been the processes operating in the liquid core of the planet.

We will consider the behavior of the main characteristics of the geomagnetic field in the vicinity of the Mesozoic-Cenozoic boundary, namely, (1) its paleointensity and variations, polarity, the frequency of its reversals and the magnitude of its direction variations, (2) the position of the Mz-Kz boundary inside the geomagnetic polarity chron C29r, and (3) the magnetic susceptibility of the World Ocean sediments.

Paleointensity

The absolute paleointensity value is usually determined using the heating techniques, known as the Thellier, Wilson-Burakov, van-Ziil, and Shaw methods [*Khramov et al.,* 1982; *Merrill and McElhinny,* 1983; *Pechersky,* 1985; and others]. Ranked as the most reliable method is that of Thellier with a necessary control of mineralogical alterations. The results of paleointensity determinations and of the dipole magnetic moments calculated from the paleointensity data have been collected in a special Database [*Tanaka and Kono,* 1994]; (BOROKRINT.MDB, 2002) and summarized in [*Pechersky,* 1998; *Shcherbakov et al.,* 2002]. According to these data, the geomagnetic field was steadily elevated in the time interval of 80–45 Ma, whereas prior to this time and after the time of 45 Ma the geomagnetic field had been two times lower for a fairly long time. In the time interval of 90–45 Ma the relative paleointensity variation ($dH_{\mathrm{a}}/H_{\mathrm{a}}$) grew from 0.1 to 0.9. Hence the Mz-Kz boundary was not recorded in paleointensity. However, the data available are not sufficient to judge about fine details. It should be emphasized that the growth of paleointensity and, especially, the abrupt growth of the paleointensity variations, began from the time of about 80 Ma, this time marking the upper boundary of the Jalal hyperchron mainly of normal geomagnetic polarity (relatively stable state of the geomagnetic field) and a transition to the hyperchron of the frequent reversals (unstable state of the field) [*Pechersky et al.,* 1983] (Figure 1a).

Geomagnetic Polarity and the Frequency of Geomagnetic Reversals

As demonstrated by the geomagnetic polarity time-scale [*Cande and Kent,* 1992], specified by E. A. Molostovsky, et al. (2004) for the Cretaceous time, the stable, mostly normal, geomagnetic polarity of the Jalal hyperchron was replaced about 80 Ma by a frequent reversals interval (Figure 1a), and the M/C boundary fitted the interval of normal polarity portion reduction. Toward the middle of the Cenozoic, by the time of the lower paleointensity, the contribution of the reversed polarity was roughly 50% (Figure 1b). Like in the case of the paleointensity, the Mz-Kz boundary is not recorded in the behavior of the geomagnetic field polarity, nor in the frequency of geomagnetic reversals (Figures 1a and 1b). Notable changes in the polarity and in the frequency of reversals was recorded at the time of about 80 Ma.

Marked lag of geological boundary from the boundary in behaviour of geomagnetic field (change of a steady-state regime of a field almost without reversals on unstable with frequent reversals) is not accidental. The similar picture is characteristic for Mesozoic-Paleozoic and Paleozoic-Proterozoic boundaries and some others, the steady regimes of geomagnetic field repeated during Phanerozoic every $\sim$100 Myr with fractal dimension about 1 (Figure 1d) [*Didenko,* 1998; *Pechersky,* 1998].

Large asteroids falling onto the Earth may contribute to its substantial shaking, which, in turn, must have affected the state of the geomagnetic field, for instance, may cause its reversal or excursion. The evidences of asteroid impacts at the time near the Mz-Kz boundary were found repeatedly, yet, no anomalies were recorded in the behavior of the geomagnetic field in the vicinity of the Mz-Kz boundary. The Mz-Kz boundary was found to reside within the C29r chron, yet, neither subchrons nor any excursions have been detected within this chron [*Cande and Kent,* 1992].

Variations of the Geomagnetic Field Direction

The total magnitude of variations in the geomagnetic field direction is controlled by its standard angular deviation $S = 81/K^{1/2}$, where K is the precision parameter of individual vector grouping in the statistical data on a sphere [*Khramov et al.,* 1982]. The same approach was used to determine the S value for the whole of the Neogea [*Pechersky,* 1998]. According to the data reported in this paper, the interval of 130 Ma to 30 Ma was marked by the slow growth of the S values from 10° to 15° with their slow decrease recorded later. These data were smoothed substantially, and the latitudinal variations of the S value was not accounted for.

Let us discuss in detail the S behavior in the vicinity of the Mz-Kz boundary. We used paleomagnetic data for time interval of 35 Ma to 140 Ma available in the Paleomagnetic Data Base GPMD-2003. This interval was chosen for the following reasons: (a) to catch the effects of any events, such as the impacts of asteroids, on the S behavior, we used an interval, for comparison, which overlapped the Mz-Kz boundary, that is, prior to, during, and after the notable impacts of asteroids onto the Earth; (b) earlier, using the examples of modern plumes, it was demonstrated that closer toward the plume epicenter the S value and its scatter grow generally, this growth being notable only for $\sim$40 million years before the onset of the igneous activity of the plume, reflecting the time of the activity in the vicinity of the core-mantle boundary, which resulted in the larger magnitude of geomagnetic field variations, on the one hand, and in the formation of a plume, on the other hand [*Pechersky,* 2001]. In this connection, we used the time interval which overlapped the potential time of the plume rising.

The data available in the Paleomagnetic Data Base were examined carefully to discard those where the number of the samples used was less than ten, where magnetic cleaning had

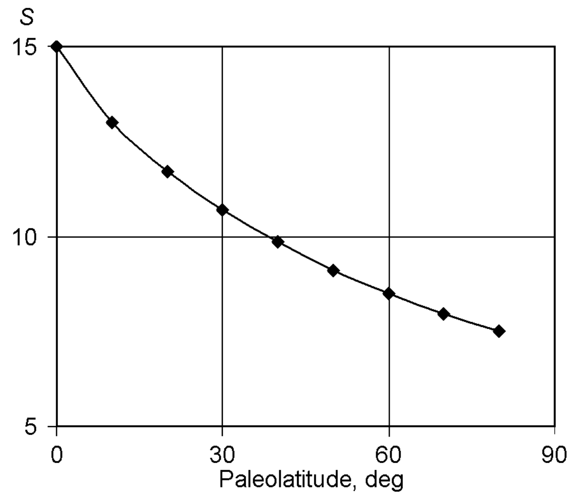

Figure 2. Empirical S variation as a function of paleolatitude [*Pechersky,* 1996]

not been performed, where the precision parameters $K < 7$ and $\alpha_{95} > 25$, and where the coordinates of the paleopole differed greatly from the average pole for a given time and a given continent. The remaining data were classified into 8 groups on the basis of their ages: 35, 55, 65, 75, 85, 100, 120, 130, and 140 Ma. The chosen age levels were actually represented roughly the ten million year intervals. Where the paleomagnetic determinations collected from the Data Base had been made for larger intervals of time, their inclusion into some or other age group was verified using the paleolatitude of the given site in the reconstructed map of the respective age. For each of the age intervals mentioned above, we used a respective map of geodynamic reconstruction prepared in terms of the program of the ODSP Plate Tectonic Reconstruction Service. Naturally, in most cases the paleolatitudes of the paleomagnetic determination site in the map and those computed from the paleomagnetic inclination turned out to be sufficiently close, although there were cases of the notably too high and too low paleolatitudes (the latter being too low for the sedimentary rocks). For this reason we preferred the latitudes which had been determined using the map.

All selected determinations were classified into four groups of the rock types: sediments, redbeds, volcanites, and intrusives. In terms of their paleomagnetic reliability all selected determinations were classified into three groups: (1) the most reliable ones, obtained using detailed qualitative magnetic cleaning, reliability tests, and other procedures, were ranked in terms of their weight as class 1; (2) the determinations of intermediate reliability were assigned the weight of 0.5; (3) the unreliable determinations, where the number of samples was less than 20, the thermocleaning was done below 400°C, using one or two temperatures, the AF cleaning was not higher than 20 mT, the reliability tests were not undertaken, these determinations were assigned the weight of 0.1. The S value showed an obvious dependence on the latitude: it decreased slowly by a factor of 2 from the equator to the pole. This behavior was observed for the intervals of the stable state of the geomagnetic field for the whole of the Neogea [*Pechersky,* 1996]. All determinations were reduced to one paleolatitude, to the latitude of the pole (S_{p}) according to dependance S from the latitude (Figure 2).

We hoped to examine the S_{p} geographical distribution for each time level. Yet, most of the data available are concentrated in the narrow zone of the Alpine-Himalayan Belt and in the Pacific Ring. For this reason we had to restrict ourselves to the analysis of the S_{p} distribution relative to the epicenters of the plumes. For each paleomagnetic dating we measured the distance along the arc of the large circle to the epicenters of two most significant plumes, close in their ages to the Mz-Kz boundary, namely; the Deccan trap basalts (their location reconstructed for the time of 65 Ma being 50°E, 20°S, which is close to the modern position of Reunion Island) and the basalts of the North Atlantic Province with their centre in Greenland (their location reconstructed for the time of 55 Ma being 330°E and 60°N, which is close to the modern position of Iceland). For comparison we used the younger Samoa Plume, with its modern position of 351°E and 14°S, and the older Rajmahal Plume, with its reconstructed ancient position of 69°E and 49°S, this being the modern position of the Kerguelen Island. It is assumed that the positions of the plume epicenters did not change markedly during the time concerned (140–35 Ma). It is believed that the beginning of the intense igneous activity of the two chosen large plumes at the earth surface was close to the Mz-Kz boundary, namely, 61 Ma (Greenland) and 65 Ma (Deccan) [*Courtillot et al.,* 2003; *Grachev,* 2000]. Judging by the estimates, available in the Paleomagnetic Data Base, the age of the basalts in the North Atlantic Province is closer to 55 Ma. The age of the Samoa Plume seems to be not higher than 20 Ma, that of the Rajmahal Plume being 118 Ma [*Courtillot et al.,* 2003].

As can be seen in Figures 3b, 3c, and 3d, the histograms of the S_{p} distribution in the sedimentary and volcanic rocks over the time interval of 75–140 Ma, excluding some unreliable determinations, are fairly close and clearly show two basic modes, $S_{\mathrm{p}} = 8°$–$9°$ and $12°$–$13°$. The relative values of the first modes for the volcanic and sedimentary rocks are very close, namely, 14.0% and 13.3%, the second mode in the volcanic rocks being similar to the first one (Figure 3b), whereas the same mode for the sedimentary rocks is more than twice lower than the first one (Figure 3c). The first S_{p} mode is also clearly seen in the histogram for the intrusive rocks (Figure 3d), yet, this group of rocks rarely show $S_{\mathrm{p}} > 10°$, the second mode of $S_{\mathrm{p}} = 12°$–$13°$ being absent (Figure 3d). This second mode "decay" in the volcanic-sedimentary-intrusive rock sequence seems to have been associated with the time during which these rocks acquired their remanent magnetization. The second mode shows its maximum value in the volcanic rocks which acquired their remanent magnetization almost instantaneously. It is partially blurred in the sediments, which acquired their remanent magnetization during for the longer time, and is not recorded in the intrusive rocks. This suggests that high-magnitude variations existed for relatively short time intervals of the unstable geomagnetic field state caused by local disturbances at the mantle-core boundary.

For the later time (65–35 Ma) the picture essentially differs from earlier time: the greater range of scattering S_p for the sedimentary and volcanic rocks (Figure 3a) is characteristic, the first mode 8°–9° is absent, and the second mode is shifted to 13°–14°. Thus, close to Mz-Kz boundary magnitude of a geomagnetic field variations appreciably grows, i.e. the regime of a geomagnetic field changes.

Let us consider the S_p variation as a function of a distance between the paleomagnetic measurement site and the epicenter of the nearest plume among those mentioned above. During the time period discussed (30–140 Ma) the continental blocks, where the paleomagnetic record had been concentrated, were located fairly far from the epicenters of all plumes, with the exception of the Greenland one. This is clearly seen in Figures 4–6, which show a very small number of the data points closer than 30°.

It should be emphasized that the distance between the epicenter of the plume and the place of its formation at the core-mantle boundary is about 3000 km, and the path along which the plume rises is often inclined, as follows from the results of seismic tomography [*Ernst and Buchan,* 2003]. The latter evidence, combined with the insufficient accuracy of determining paleomagnetic directions and paleomagnetic reconstructions, results in the fact that the S_p values obtained for the Earth surface distances measuring a few tens of degrees are notably scattered and little depend on the distance to the plum epicenter. We would remind that each age level is actually an interval of about ten million years. Consequently, in our case of the uncertain distance from the plume source, a uncertain time of the unstable state at the core and mantle boundary, and consequently, of the unstable state of the geomagnetic field, the approach to the plume epicenter must be expressed, first, in the growth of the variation magnitude, that is, in S_p variation and, secondly, in the growth of the S_p scatter. Moreover, the presence of other plumes of different ages acting during the time period concerned may disturb the S_p distribution relative to the four epicenters of the plumes. For example, at least ten modern lower mantle plumes have been reported [*Courtillot et al.,* 2003; *Ernst and Buchan,* 2003; *Grachev,* 2000]. In addition to the above reasons, we should not forget the technical errors, inaccurate measurements, not always correct identification of the primary NRM components (the presence of stable secondary components), and other factors, each of them being responsible for the scatter of S_p individual values. Only their mean values and their standard deviations can be ranked as objective quantitative characteristics.

Let us go in age time from above to downwards.

Level for 35 Ma (the real age interval of ~25 Ma to 45 Ma) (Figure 3a, Figures 4–6, Table 1). This time interval is characterized by a large S_p scatter from about 3° to 20° and by the large standard deviation (±4.8°) irrespective of the distance from the plumes. The mode is 13°–14° (Figure 3a), the S_p distribution is asymmetric; as a result, the average S_p = 9.9° (Table 1), being shifted to the left relative to the mode, resting between the first and second modes (Figures 3b and 3c).

Level for 55 Ma (the real age interval of ~50–62 Ma) (Figure 3a, Figures 4–6, Table 1). The S_p behavior is similar to that of 35 Ma; the S_p value varies from 4° to 22° and does not depend on distances to the plumes. The average S_p of 11.5° (see Table 1) coincides with that of the second mode (Figures 3b and 3c).

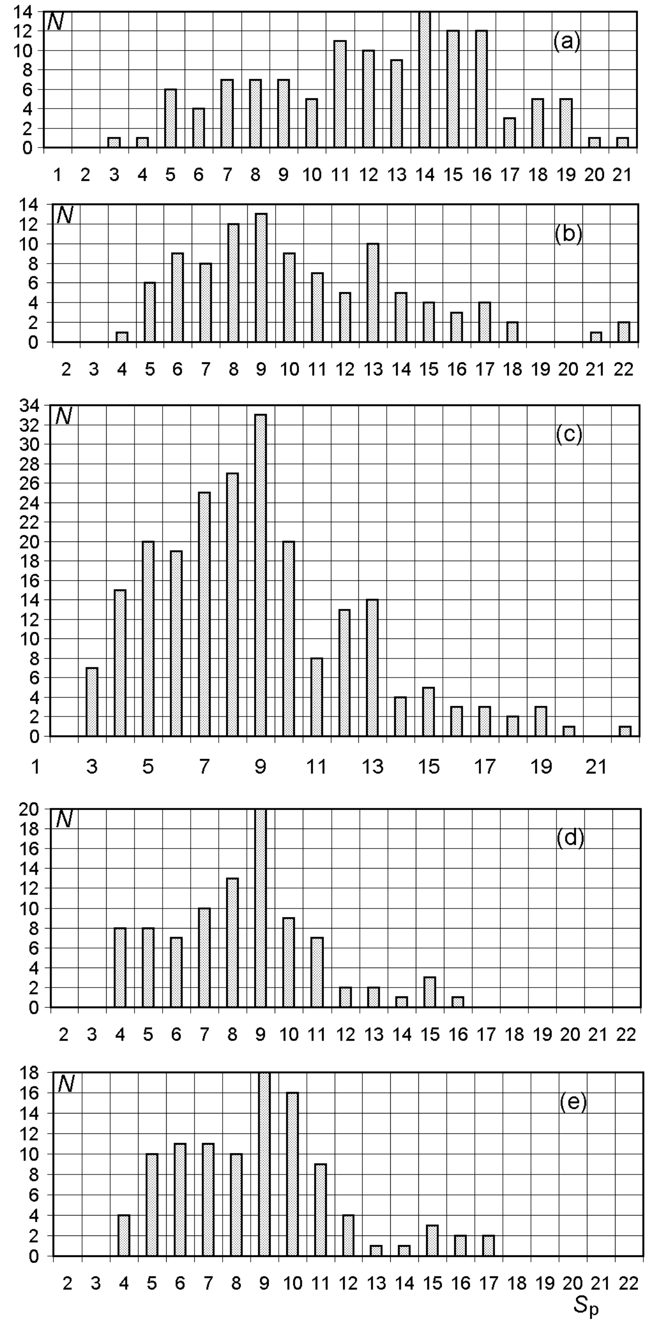

Figure 3. Histograms of S_p distribution for rock groups and different ages, plotted for the most reliable paleomagnetic data (Groups 1 and 2, see the text): (a) volcanic rocks and sediments, 35–65 Ma; (b) volcanic rocks, (c) sediments, including red beds, (d) intrusive rocks, (e) volcanic rocks and sediments, remote from the epicenters of the plumes for distances of > 60°, their ages (b, c, d, and e) ranging from 75 Ma to 140 Ma.

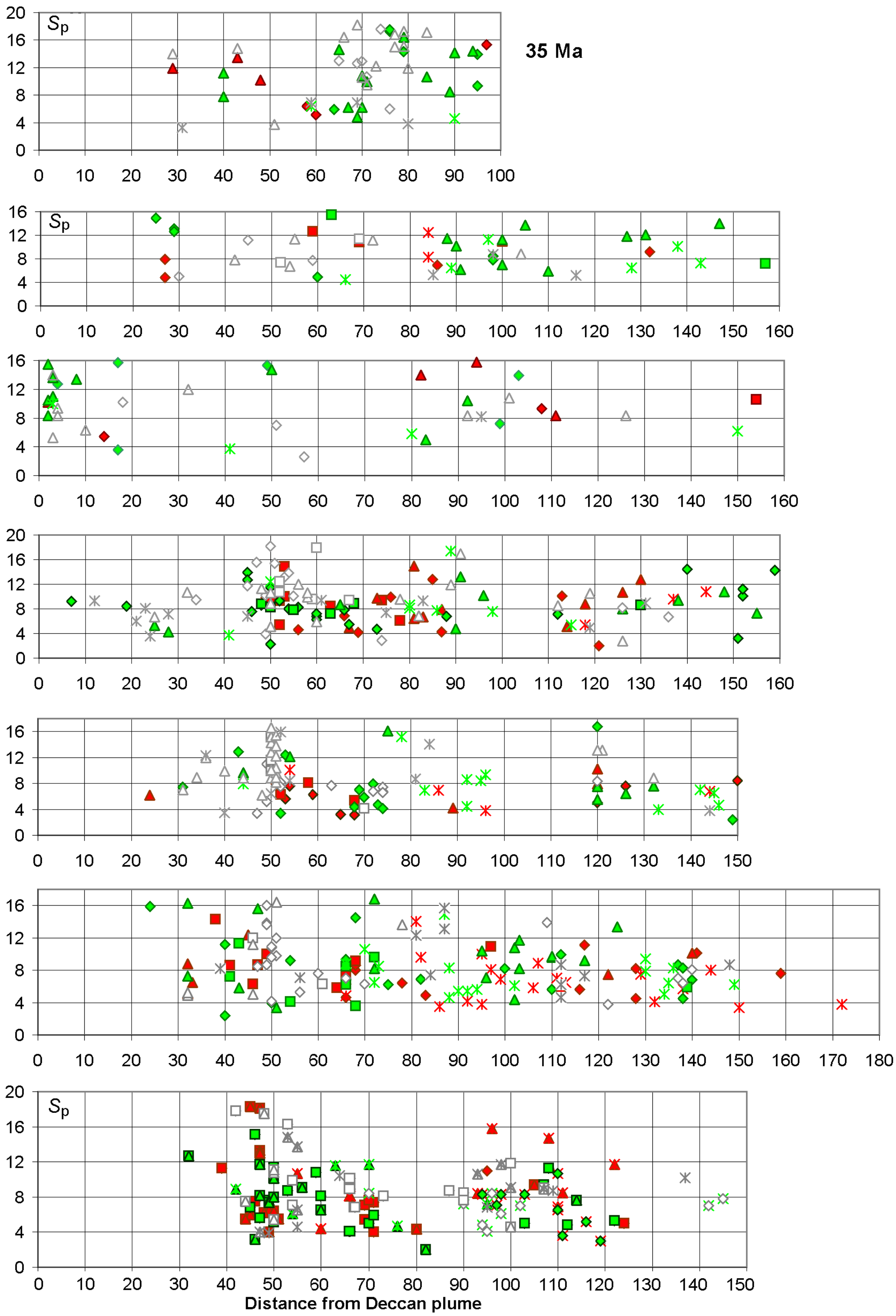

Figure 4. The S_p distribution as a function of the distance to the Deccan Plume epicenter. The rhombs denote the sediments; the squares, the red sediments; the triangle, the volcanic rocks, and the stars, the intrusive rocks. Shown in red color are the most reliable paleomagnetic data, the green, less reliable, and the gray, unreliable (see the text).

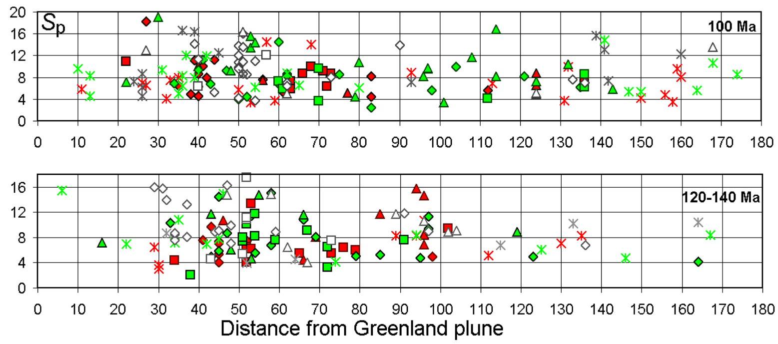

Figure 5. The S_p distribution as a function of the distance from the Greenland Plume epicenter. The rhombs show the sediments; the squares, the red sediments; the triangles, the volcanic rocks, and the stars, the intrusive rocks. The red color shows the most reliable paleomagnetic data, the green color, less reliable, and the gray, the unreliable data (see the text).

Level for 65 Ma (the age interval of ~63–72 Ma) (Figure 3a, Figures 4–6, Table 1). Similar to the sections for 35 Ma and 55 Ma, the S_p behavior is independent of the distances to the plumes. It varies from 2° to 16°–19°, the average S_p and its standard deviation is similar to that observed for the level of 55 Ma, see Table 1.

Level for 75 Ma (the age interval of ~73–82 Ma) (Figures 3b and 3c, Figures 4–6, Table 1). In relation to the Deccan plume the dependence on distance up to its epicenter has not observed. With the exception of some occasional kicks (Figure 4), the S_p values fit in the interval of 3–15°, the average value of 9° coincides with the first mode (Figure 3b and c), the standard deviation value diminishing to ±3° (Table 1). An absolutely different pattern was observed in the case of the Greenland plume. At a distance from this plume, the S_p value corresponds to that of the first mode (average $S_p = 8.4°$), the dispersion being as low as ±2.2° (Figure 5 and Table 1). Closer to the Greenland Plume, the average S_p value grows to 12° (second mode), its scatter being from 2° to 22°, the standard deviation growing to ±4.2° (Figure 5, Table 1).

Level for 85 Ma (the age interval of ~83–94 Ma) (Figures 3b and 3c, Figures 4–6, Table 1). The average S_p values for both plumes are at the level of the first mode, yet, show a significant scatter in the magnitude values, the scatter being 4°–10° at distances greater than 60°, and growing to 2°–17° closer to the epicenters of the plumes in both cases.

Level for 100 Ma (the age interval of ~95–110 Ma) (Figures 3b and 3c, Figures 4–6, Table 1). In compari-

Table 1. Average weighted magnitude of paleomagnetic direction variations (S_p) as a function of the distance to the plume epicenter

Time, Ma	Distance <60°	Distance >60°	Av. S_p
35 (25–45)	9.9±4,8 (75)	10.3±4 (22)	10±4.6
55 (50–62)	11.5 (62)	11.9 (18)	11.6±4.1
65 (63–72)	11.8 (40)	11.3 (16)	11.6±4.2
75 (73–82)	12±4.2 (Greenland, 122); 9±3 (Deccan, 55)	8.4±2.2 (26)	10.8±4
85 (83–94)	8.5±4 (Greenland, 103); 7.7±4,5 (Deccan, 162); 8.5±3.4 (Samoa, 17)	it is not enough of the data	8±4
100 (95–110)	8.5±3.5 (Greenland, 84); 11.5±4.6 (Deccan, 49); 6.6±2.5 (Samoa, 16)	7.8±3.1 (44)	8.9±4
120–140 (112–145)	8±3.5 (Greenland, 68); 9.4±3.8 (Deccan, 49); 5? (Samoa, 2)	8.4±2.9 (38)	8.5±3.5

Note: Time – age level and interval for paleomagnetic data; Distance – average weighted S_p for distance to plume epicenter on an arch of a large circle, smaller or greater 60°, ±standard deviation; the number of S_p determinations is given in brackets Av. S_p – average weighted S_p for for all paleomagnetic determinations irrespective of distance to plume epicenter.

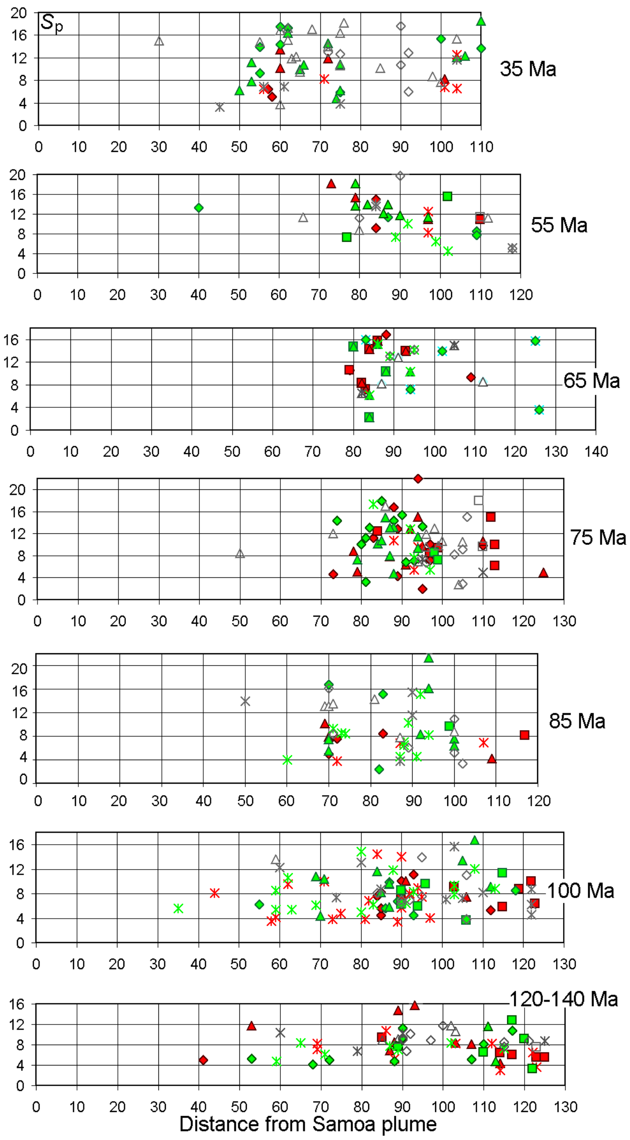

Figure 6. The S_p distribution as a function of the distance to the Samoa Plum epicenter. The rhombs denote the sediments; the squares, the red sediments; the triangles, the volcanic rocks; the stars, the intrusive rocks. Shown in red are the most important paleomagnetic data, those in green are less reliable data, the gray color denoting the unreliable data (see the text).

son with level 85 Ma the S_p disorder begins to be felt in the Deccan case on distances more than 100° and with approach to plume reach 3°–16° (Figure 4), thus average S_p corresponds to the second mode (11.5°, Figures 3b and 3c) and standard deviation is ±4.6° (Table 1). In a case of Greenland plume such tendency practically is absent, that is seen on average S_p, which corresponds to the first mode and rather small standard deviation of S_p (Table 1).

Level for 120–140 Ma (the age interval of ∼112–145 Ma) (Figures 4–6, Table 1). Only 17 and 18 determinations were made for the ages of 130 Ma and 140 Ma, respectively, 13 of them showed a low paleomagnetic reliability. For this reason they are not considered separately, but are included into this interval. The S_p scatter is 3°–18° as approaching to Deccan plume epicenter, but is less conspicuous compared to the level for 100 Ma (Figure 4). This is manifested in the average value and standard deviation of S_p (Table 1). In the case of the Greenland plume the scatter is lower (2°–15°), and the S_p value almost does not grow closer to the plume epicenter (Figure 5). This is proved by the lower S_p value, 8.5°±3.5°, coinciding with the first mode (Figures 3b and 3c, Table 1).

None of the levels showed any tendency of the S_p growth in the direction to the Samoa plume epicenter (Figure 6 and Table 1), this proving the age of the plume to be younger than 25 Ma.

None of the levels showed any trend of the S_p growth in the direction toward the Rajmahal plume except for the period of 130–140 Ma, yet the data for this period of time are scarce and belong to the area spaced at a distance of more than 50° from the Rajmahal. It can be supposed that some S_p growth, which begins to show in this interval of time, in the direction toward the Deccan plume epicenter, is actually associated with the Rajmahal plume, the epicenter of which resides relatively close to the Deccan plume epicenter.

The possibility that some other plumes, unaccounted for, might have affected the S_p behavior was tested in the following way: using Figures 4 and 5, we chose the points of relatively high S_p values for each time section, their distances to the epicenters of the two plumes are listed in Table 2. Then, we drew circles from the plume epicenters, the radii of which were equal to the distances to the sites of high S_p values; the coordinates of their intersections are also listed in Table 2. These intersection points might be the epicenters of the plumes. However, the coordinates of these intersections, listed in Table 2, do not coincide with any of the epicenters of the known lower mantle plumes, for instance, of those reported by *Courtillot et al.* [2003]. It is possible therefore that these are some random S_p "jumps", unrelated to the plume formation process.

Discussion of Results

The two-mode S_p distribution over the time interval of 75–140 Ma is a regional effect: the second (higher) S_p mode exists only at relatively small distances from the Greenland and Deccan plume epicenters in the age interval of 75–140 Ma (Figures 3b and 3c). Away from the plume epicenters, the higher S_p mode disappears, which is clearly shown by a histogram (Figure 3e) and confirmed by the average S_p values (Table 1). At the same time the first S_p mode for the time interval of 75–140 Ma and the respective weighted average S_p value exist irrespective of the distances to the epicenters of the plumes. Consequently, during the 75–140 Ma, the average magnitude of variations in the geomagnetic field direction was 8°–8.5°. This can be ranked as a global effect characterizing the ordinary state of the geomagnetic field which was predominantly of normal polarity. This background was superimposed by some anomalous geo-

Table 2. Points of crossing of distances raised S_p to the Deccan and Greenland plume epicenters

Time, Ma	Deccan (50°E, −20°S)	Greenland (−30°W, 60°N)	Longitude	Latitude
35	78°	55°	−16°W	10°N
75	52°	75°	3°E	−5°S
75	85°	32°	−10°W	33°N
75	85°	75°	−37°W	−15°S
85	52°	72°	3°E	−5°S
100	50°	52°	32°E	32°N
120–140	45°	95°	8°E	−28°S
120–140	108°	95°	−71°W	−28°S
120–140	108°	52°	−52°W	13°N

Note: Deccan and Greenland – the disnance on an arch of a large circle of the raised S_p to one of plume epicenters (see Figures 4 and 5). Longitude and Latitude – coordinates of points crossing.

magnetic field of the locally regional character. This anomalous state was obviously caused by some local disturbances in the ordinary state of the geomagnetic field in the regions of the Greenland and Deccan plume generation. Worthy of note is the excellent similarity of the histograms presented in Figures 3d and 3e, even though the former was plotted for the intrusive rocks and the latter for the lavas and sedimentary rocks. This proves that at great distances from the plume epicenters, both the long-tern (intrusive rocks) and short-term (lavas) paleomagnetic data record only the ordinary state of the geomagnetic field.

The above-mentioned "degradation" of the second S_p mode in the volcanic-sedimentary-intrusive rock sequences (Figures 3b, 3c, and 3d) seems to have been controlled by the duration of the time during which the rocks acquired their remanent magnetization (this mode has a maximum value in the volcanic rocks, which acquire NRM almost instantaneously, and disappears in the intrusive rocks, where the NRM acquiring is considerably extended in time). This proves the short life of high-magnitude anomalous variations during the short interval of the unstable-state geomagnetic field caused by local disturbances at the core-mantle boundary, which lead to the formation of plumes. The relatively short existence of high-magnitude variations is proved by the greater scatter of the S_p values in the vicinities of the Deccan and Greenland plume epicenters, each of the levels concerned containing the values for the intervals of about 10 million years. The short-term anomalous field magnitude variations and plume formation are proved by the following fact. Moving closer to the modern global magnetic anomalies, we observe a similar growth in the field variation magnitude, the life time of the global anomalies is proved by these data to be less than 20 kyr [*Pechersky,* 2000, 2001]. This suggests a close relationship between the sources of world magnetic anomalies and plume formation and, hence, the short life of both.

The most significant anomalous "splash" in the field direction variation magnitude, associated with the Greenland plume, was dated about 80 Ma, the duration of this plume rise, being about 20 million years. In the case of the Deccan plume, the anomalous "splash" of the geomagnetic field variation, associated with this plume, was dated ∼100 Ma. Hence, the rising of the Deccan plume lasted about 35 million years.

Therefore, we have a kind of paradox here: the formation of plumes and disturbances in the core, which result in the growth of geomagnetic field variations, are closely associated with one another, yet, the disturbances in the top of the liquid core and, hence, in the geomagnetic field variation, are relatively short events, whereas the high activity of the two plumes discussed lasted approximately 80–100 million years. It can be supposed that the disturbance at the core-mantle boundary, which resulted in the growth of the geomagnetic field variations and in the formation of a plume, attenuated rapidly in the core, yet, the hot spot at the base of the mantle might have existed for a hundred million years, similar to magma chambers in the crust, where large intrusion chambers are known to live off for millions of years.

Approximately close to the Mz-Kz boundary a fluctuation level of the geomagnetic field direction variation appreciably changes: on the average from 8°–8.5° to 11.6° (Table 1), this rise being of a global scale. Unfortunately, the large "window" of dating the paleomagnetic results does not allow to state that the sudden growth in the field variation magnitude had taken place at the Mz-Kz boundary. However, we can trace a regular change in the medium-size variations, showing its global character: during the Cretaceous the trend of the geomagnetic field was fairly stable, its average value being 8°–8.5°; it was almost not affected by the substantial reconstruction which took place in the core ∼80 Ma, which was responsible for a change in the polarity and in the reversal frequency of the geomagnetic field; beginning from the time of about 65 Ma, the average variation level increased to 11.6°, remained the same for the period of roughly 20–25 million years, declined slowly to 10° 35 Ma, and continues to decline (Figure 1c, Table 1). Thus, a global change took place in the liquid core, responsible for the geomagnetic field direction variations, at the boundary between the Mesozoic and Cenozoic. It follows that two different regimes operate in the core: one of them being responsible for the reversals and polarity, the other, for variations of the direction of the geomagnetic field.

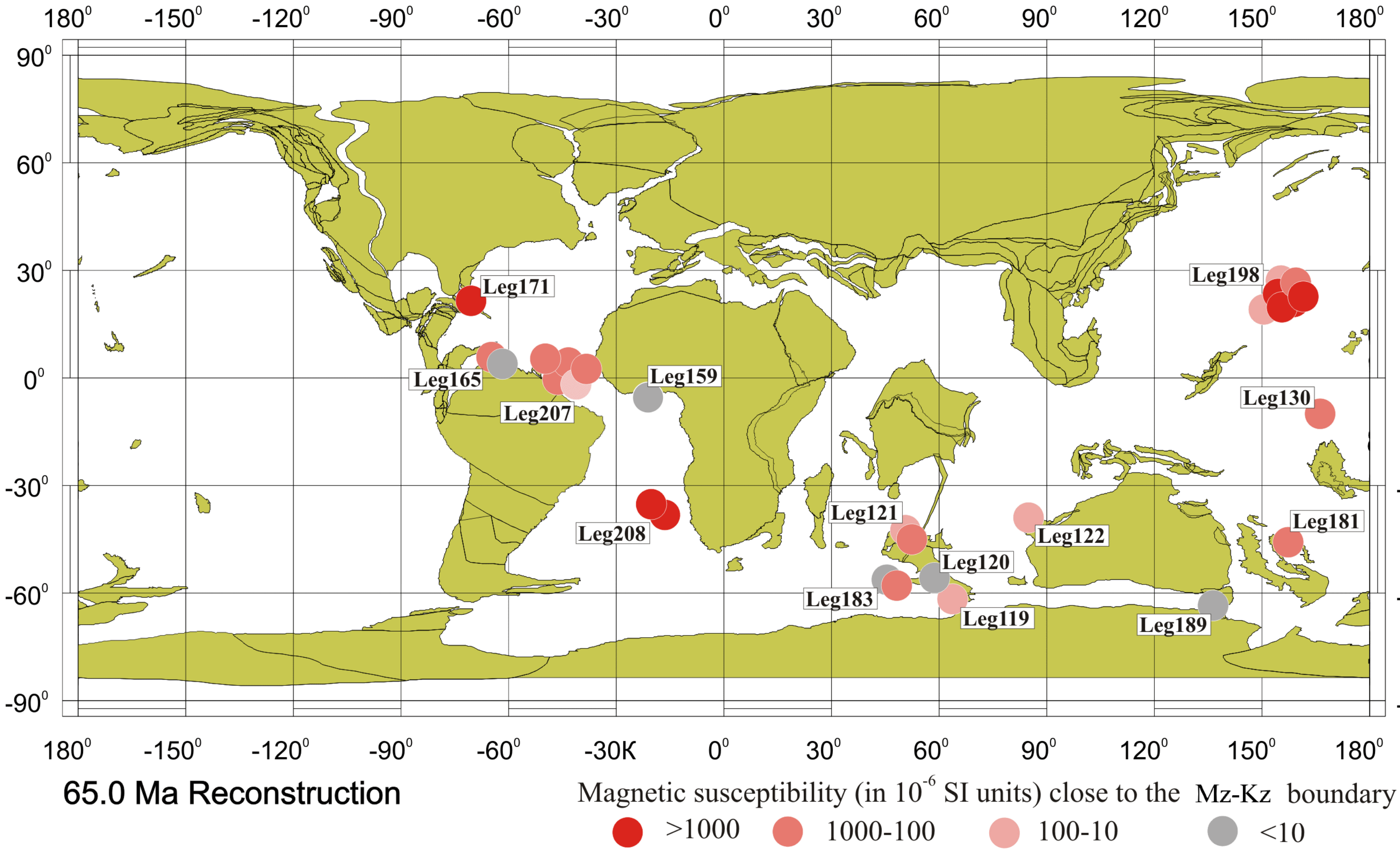

Figure 7. The κ-peak distribution in the oceanic sediments in the vicinity of the Mz-Kz boundary, the map is reconstructed for the time of 65 Ma. The bright red circles show intensive κ-peaks with $\kappa > 1000 \times 10^{-6}$ SI units; the red circles show the intermediate κ-peaks, $100 < \kappa < 1000 \times 10^{-6}$ SI units; the pink circles denote small κ-peaks, $10 \leq \kappa \leq 100 \times 10^{-6}$ SI units; the grey circles denote that the κ-peak is either absent or is lower than 10×10^{-6} SI units. The numbers near the circles denote the number of the DSDP and ODP leg.

Magnetic Susceptibility in the Oceanic Sediments in the Vicinity of the Mz-Kz Boundary

Collecting data for the sections of oceanic sediments, we can trace, in space and time, the distribution of the magnetic susceptibility (κ-peak), recorded by a number of investigators, and verify the global character and synchronism of this event, and its association with the Mesozoic-Cenozoic biostratigraphic boundary. For this purpose we carried out the following work. At the first stage of our work, using the volumes of the DSDP and ODP Initial and Scientific Reports, we selected the holes drilled in the sedimentary rocks underlying the ocean floor, which, as stated by the authors, first, included the Mz-Kz boundary and, secondly, presented a continuous sequence in the time interval which was of interest for us. At the second stage of our work we selected from these holes the following information: the position of the Mesozoic-Cenozoic biostratigraphic boundary in the section of the hole, the presence or absence of the κ-peak, its value, width (thickness in the section), and position relative to the Mz-Kz boundary. The Mz-Kz boundary, dated 65 Ma, and, hence, the κ-peak, closest to it, were located within the reversed polarity chron C29r. Proceeding from the fact that the sequences concerned are wholly or fairly continuous (except for very short gaps, as in the 1135a hole), we assumed that most of the sections we collected represented the C29r magnetochron fairly well (except for 1138a hole, where the thickness of the sediments, corresponding to the C29r chron is only 3 m).

Accordingly, where we managed to find any good magnetostratigraphic information, the data described above were referred to the time. Where magnetostratigraphic data were lacking, the time length of the κ-peak was estimated using the thickness of the sediments corresponding to the C29r chron, namely, $\sim$10 m. This is rather free assumption, but it allows judge about the time during which magnetic material had accumulated in the vicinity of the Mesozoic-Cenozoic biostratigraphic boundary, at least in the range of the order. As follows from the geomagnetic polarity time-scale [*Cande and Kent,* 1992], the duration of the C29r chron was 0.833 Ma, the relative distance between the Mz-Kz boundary and the lower boundary of the chron being 0.69. These figures will be used below. Gathered data are listed in Table 3 and plotted in the map of paleoreconstruction for 65 Ma (Figure 7).

It follows from Table 3 and Figure 7 that in four sections any notable changes of susceptibility at the Mz-Kz boundary are absent. Three columns more should be added to this list, where the $\kappa_{\max}$ values are not higher than 10^{-5} SI units. Neither the distribution of the κ-peak, nor its value vary with distance from the nearest land (Figure 7), i.e. with the distance from the source areas of the sediments. On the contrary, the rocks which do not show any κ-peak seem to be located not far from the continents. The κ-peak value varies widely from 10 to $> 2000 \times 10^{-6}$ SI units (Table 3), being in agreement with the lithology and, especially, with variations of the iron content in the sediments. The highest κ-peak values, such as, 600×10^{-6} SI units (Hole 752), $1000–1300\times10^{-6}$ SI units (Holes 1209–1211), and $1200–2500\times10^{-6}$ SI units (Holes 1262-1267) are located near the epicenters of the active plumes Kergelen, Hawaii, and Walvis Ridge, respectively. It would be interesting to trace variations in the κ-peaks with distance from the epicenters of the plumes that had been active 65 million years ago, as it was done for the magnitude of the field direction variation (see the previous section of the paper), yet, the data available are too scarce.

It is important to emphasize that the κ-peaks recorded in the vicinity of the Mz-Kz boundary are not unique or anomalous ones, being a common phenomenon for oceanic sediments, including Late Cretaceous and Paleocene sediments. Moreover, the κ-peaks recorded in the sediments unassociated with the Mz-Kz boundary often more intensive (Figure 8). The κ-peaks vary significantly in width (Figure 8): from 10 cm (Hole 1212a) to 9 m (Hole 758a). These widths do not correlate with the sedimentation rate, but reflect different interval of time, when the sediments were enriched in magnetic materials, varying from <10 kyr to $\sim$0.7 Myr, the most common intervals being a few tens of thousand years (Table 3, Figure 8). Most of the κ-peaks were symmetrical, the asymmetrical ones being rare. In the latter case the susceptibility value declined much slower after $\kappa_{\max}$, compared to the susceptibility growth to $\kappa_{\max}$ (Figure 8).

Table 3 shows that the position of the κ-peak varies greatly relative to the Mz-Kz boundary: (1) as has been mentioned above, seven of the examined sections did not show κ-peaks at all, or those present ones were lower than 10^{-5} SI units; (2) the Mz-Kz boundary was recorded at the beginning of the κ-peak growth in 8 holes; (3) the Mz-Kz boundary was inside the κ-peak interval, but lower than the $\kappa_{\max}$ values in 4 holes; (4) the Mz-Kz boundary coincided with $\kappa_{\max}$ values in 11 holes, and (5) the Mz-Kz boundary was found to be lower than the κ-peak interval in three holes. These data and the above information prove that there is no direct relationship between the substantial changes in the organic world and the accumulation of iron in the oceanic sediments in the vicinity of the Mz-Kz boundary. This seems to have been a coincidence of two different processes.

Let us discuss the important problem of the global synchronism of the Mz-Kz biostratigraphic boundary and, hence, that of the κ-peaks, which is emphasized by many researchers [*Ellwood et al.,* 2003]. First, we will examine the positions of the Mz-Kz boundary and κ-peaks inside the C29r chron. Discarding the data for the 1138a core, where the thickness of the C29r chron is too low (probably because of many gaps in the sedimentation or because of erosion), the thickness of the C29r chron varies from 7 m to 12 m (Table 3). Proceeding from the geological evidence and relatively low thickness variations, we can admit that sediments accumulated in these columns without any notable gaps and, consequently, embraced the time equal to the duration of the C29r chron, and that the time intervals during which these sediments accumulated were synchronous, since the C29r magnetochron is a global marker of their synchronism. The Mz-Kz biostratigraphic boundary varies in its position inside the C29r chron (Table 3), being asynchronous in the World Ocean basin, and was obviously controlled by the paleolatitude (Figure 9). This is especially obvious if we

Table 3. Information on κ-peak near to the Mz-Kz boundary and its position inside the chron C29r

leg	hole	Plat.	Mz-Kz, mbsf	C29r, thick.	Mz-Kz position	κ-peak, mbsf	κ-peak beginning, mbsf	κ-peak end, mbsf	κ-peak length	κ_{max}, 10^{-6} SI units
113	690c	−65°S	248.2	4.8	0.88	no infor.				
119	738c	−62°S	377.1			376.9	377.1	376.7	~0.033	10
120	750a	−57°S	350.1			350	350.08	349.66	~0.036	7.5
121	752b	−44°S	357	9	0.78	356.7	358.5	354	0.43	600
121	758a	−42°S	295.6	~11	~1.0	295	297	288	~0.72	50
122	761b	−40°S	176.4	7	0.8	absence				
122	761c	−40°S	173.3			172.5	172.5	172.4	~0.008	21
122	762c	−40°S	554	5	0.8	no infor.				
130	807c	−10°S	1197.5	8	0.25	1197.2	1197,1	1197,2	0.01	100
159	959d	−7°S	866			absence				
165	1001a	5°N	352,2	5.3	0.59	absence				
165	1001b	5°N	352.9			352.9	353.1	352.8	~0.026	75
171	1049a	21°N	126.08	6	0.16	124	125.1	124.67	0.07	280
171	1050c	21°N	405	9	0.29	no infor.				
181	1124c	−50°S	466			466	466.9	462	~0.4	800
183	1135a	−57°S	260.2	~11	0.94	260.1	261	259.9	0.086	6.5
183	1138a	−58°S	490			490	491	489	~0.167	180
189	1172d	−64°S	715			absence				
198	1209a	22°N	235.3			235.3	235.5	235.1	~0.033	1100
198	1209c	22°N	234.9			234.9	235.2	234.8	~0.033	1150
198	1210a	20°N	219.8			219.9	220.15	219.7	~0.037	1000
198	1210b	20°N	219.7			219.7	219.9	219.6	~0.024	1380
198	1211a	20°N	133.5?			133.8?	134	133.5	~0.04	400
198	1211b	20°N	133.7?			133.7	134	133.4	~0.05	1030
198	1211c	20°N	133			133	133.3	132.9	~0.033	1300
198	1212a	23°N	109			109	109.05	108.95	~0.009	75
198	1212b	23°N	101.45			101.45	101.6	101.3	~0.043	60
207	1258a	1°N	275			273	280	270	~0.8	200
207	1259a	1°N	444.5			442.5	444	441	~0.25	170
207	1259b	1°N	444			442.5	444	441	~0.25	175
207	1260a	1°N	333			332.5	333	331	~0.167	70
207	1260b	1°N	333			332.5	333	331	~0.167	100
208	1262b	−37°S	195.53	5–8	0.66–0.81	195.7	195.53	195.2	~0.04	2500
208	1262c	−37°S	196.68	7–12	0.76–0.86	196.9	196.68	196.3	~0.04	2500
208	1267a	−38°S	320	~10	~0.8	320	320.5	316	~0.33	1200
208	1267b	−38°S	300	~10	~0.7	300	300.5	296	~0.33	1200

Note: leg – number of leg; hole – number of hole; Plat. – paleolatitude of hole, paleoreconstruction on 65 Ma; Mz-Kz – position of biostratigraphic boundary of Mesozoic and Cenozoic in section (depth from a surface of the ocean bottom in m); C29r, thick. – the thickness of magnetochron C29r in m; Mz-Kz position – the position of Mz-Kz biostratigraphic boundary in regard to lower boundary of chron C29r; κ-peak – position of the nearest to Mz-Kz κ-peak in section, in m; absence – κ-peak is absent; κ-peak length – duration of κ-peak (Myr); κ_{max}‘– the maximal value of κ-peak, 10^{-6} SI units. ~ the doubtful results are marked.

compare the pairs of holes in which the C29r chron has the same thickness. Hence, here we deal with the identity of the time records: the examples are Hole 752b (the C29r chron thickness is 9 m, the Mz-Kz boundary position is 0.78) and Hole 1050c (9 m and 0.29, respectively); Hole 761b (7 m and Mz-Kz boundary position of 0.8), and Hole 1049a (7 m and 0.16, respectively). Differences in the positions of the Mz-Kz boundary amount to 0.7 Myr between the south of the southern hemisphere and the northern hemisphere (Figure 9, Table 3).

Conclusion

The events listed in the Introduction, which had taken place at the surface of the Earth were not synchronous. Their correlation is not so obvious, that demonstrate the reviews [*Ernst and Buchan,* 2003; *Veimarn et al.,* 1998] and suggested in this paper. To what extent the paleomagnetic events described in this paper were associated with them?

(1) Considering the paleomagnetic events, we can speak

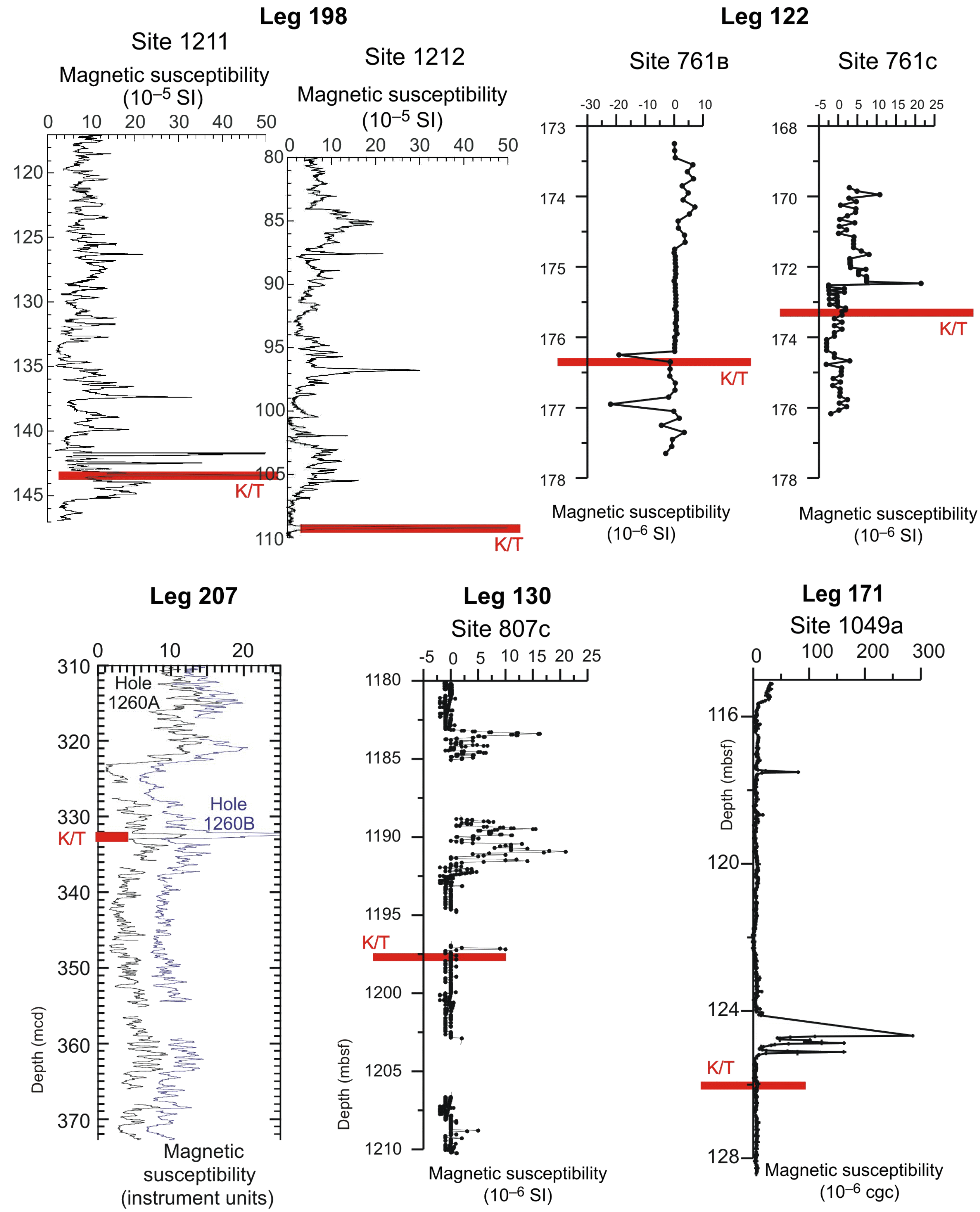

Figure 8. The examples showing the behavior of the magnetic susceptibility of oceanic sediments in the vicinity of the Mesozoic-Cenozoic boundary.

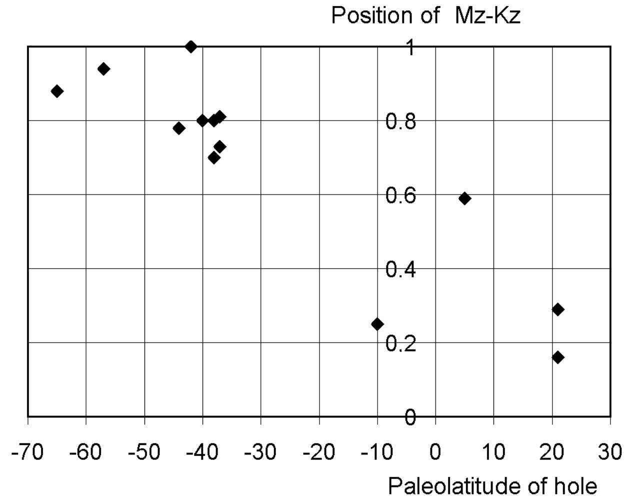

Figure 9. Variation of the relative position of the Mz-Kz boundary inside the C29r chron as a function of the paleolatitude of the oceanic sediment section (hole).

only about a change in their variation conditions, which occurred at the boundary between the Mesozoic and Cenozoic eras, this being a fairly far fetched deduction because of the highly indefinite age of the primary natural remanent magnetization component. The global character of this event suggests some general change in the generation of the geomagnetic field variation in the vicinity of the Mesozoic-Cenozoic boundary.

(2) The change in the Earth core regime, responsible for the geomagnetic field reversals began notably earlier than 65 Ma, i.e. a change in the latter was not associated with the Mz-Kz boundary. But marked lag of geological boundary from the boundary in behaviour of geomagnetic field (change of a steady regime of a field almost without reversals on unstable with frequent reversals) was not accidental. The similar picture is characteristic for Mesozoic-Paleozoic and Paleozoic-Proterozoic boundaries, the steady regimes of geomagnetic field repeated during Phanerozoic every ~100 Myr.

(3) Variations in the geomagnetic field direction remained the same prior to and after a change in the reversal regime. Consequently, these two regimes of the geomagnetic field generation were not connected with one another.

(4) The local changes in the magnitude of the magnetic field variations were associated with the formation of plumes in the vicinity of the core-mantle boundary. Yet, speaking about the plumes, which were active at the Earth's surface in the vicinity of the Mz-Kz boundary (for example, the plumes of Greenland and Deccan), they originated 20–35 million years earlier than the Mz-Kz boundary. It is possible, in terms of paleomagnetic data, this result indicate the relationship between biota extinctions and plume igneous activity on the Earth surface, and lag between the beginning of plumes near the core/mantle boundary and the Mz-Kz boundary reflects the time of plume raising.

(5) In fact, the Mz-Kz boundary is often, yet not necessarily, marked by a peak of magnetic susceptibility, that is, the latter is not a characteristic of the Mz-Kz boundary. The highest κ-peak values are close to the epicenters of the active plumes, yet the $\kappa_{\max}$ values are not unique even in the vicinity of the plumes, some higher values have been observed far from the epicenters of the active plumes. The process of magnetic material accumulation in the sediments lasts from a few dozens of years (most commonly) to hundreds of thousand years. Where this interval (κ-peak) is observed, it varies in its disposition relative to the Mz-Kz boundary; it often includes the Mz-Kz biostratigraphic boundary, and $\kappa_{\max}$ resides above it. Moreover, the Mz-Kz biostratigraphic boundary marking a change in the biota in the World Ocean is not synchronous one, but varies with the paleolatitude. For instance, the difference in the positions of the Mz-Kz biostratigraphic boundary in the south of the southern hemisphere and in the northern hemisphere amounts to 0.7 million years.

(6) As follows from the data discussed in this paper, it would be more correct to speak not of a discontinuous jump in the processes, but of a considerable time interval of changes in the vicinity of the Mz-Kz boundary. It appears that the events situated near the Mesozoic-Cenozoic boundary are related only to the upper part of the Earth, such as, the lithosphere and the surface of the Earth, but there are synchronous the events in the core or at its boundary with the mantle, such as magnitude of geomagnetic field direction variation. As indicated earlier [*Pechersky,* 1998], this association reflects the existence of some external mechanism common for the processes operating in the core and at the surface of the Earth. Acting as "triggers" might have been the impacts of large asteroids to the Earth surface, which might have caused, for example, a global change in the magnetic direction variation. Yet, the impacts of this kind did not have any effects on the geomagnetic field reversals or on the formation of the plumes near Mz-Kz boundary.

Acknowledgments. We are thankful to K. Popov and Z. Sharonova for their help in collecting data. This research was supported by Program 5 of the Earth Science Division of the Russian Academy of Sciences.

References

Alvarez, W., A. Asaro, and A. Montanari (1990), Iridium profile for 10 million years across the Cretaceous-Tertiary boundary at Gubbio (Italy), *Science, 250,* 1700–1703.

Baulus, B., D. R. Peacor, and W. C. Elliot (2000), Coexisting altered glass and Fe-Ni oxides at the Cretaceous-Tertiary boundary, Stevens Klint (Denmark): Direct evidence of meteorite impact, *Earth Planet. Sci. Lett., 182,* 127–136.

Cande, S., and D. V. Kent (1992), A new geomagnetic polarity timescale for the Cretaceous and Cenozoic, *J. Geophys. Res., 97,* 917–932.

Courtillot, V., A. Davaille, J. Besse, and J. Stock (2003), Three distinct types of hotspots in the Earth's mantle, *Earth Planet. Sci. Lett., 205,* 295–308.

Didenko, A. N. (1998), Paleozoic 100 Myr variations of processes in the core and lithosphere, *Physics of the Earth,* (5).

Ellwood, B. D., W. D. MacDonald, C. Wheeler, and S. L. Benoist (2003), The C-T boundary in Oman: Identified using magnetic susceptibility field measurements with geochemical information, *Earth Planet, Sci. Lett., 206,* 529–540.

Ernst, R. E., and K. L. Buchan (2003), Recognizing mantle plumes in the geological record, *Annu. Rev. Earth Planet. Sci., 31,* 469–523.

Grachev, A. F. (2000), Mantle plumes and the problems of geodynamics, *Physics of the Earth,* (4), 3–37.

Jurdy, D. M., M. Stefanick, and C. R. Scotese (1995), Paleozoic plate dynamics, *J. Geophys. Res., 100,* 17,965–17,975.

Khramov, A. N., G. I. Goncharov, R. A. Komissarova, et al. (1982), *Paleomagnetology,* 312 pp., Nedra, Leningrad.

Merrill, R. T., and M. W. McElhinny (1983), *The Earth's Magnetic Field,* 401 pp., Academic Press, London.

Montanari, A., S. Bagatin, and A. Farinella (1998), Earth cratering record and impact energy flux in the last 150 Ma, *Planet. Space Sci., 46,* 271–281.

Pechersky, D. M. (1985), *Petromagnetism and Paleomagnetism,* 128 pp., Nauka, Moscow.

Pechersky, D. M. (1996), Variation of the total magnitude of the geomagnetic field direction as a function of the latitude in Neogea time, *Geomagnetism and Aeronomy, 36*(5), 130–136.

Pechersky, D. M. (1998), Neogea paleomagnetism constraints on the processes in the core and at the surface of the Earth, *Russian J. Earth Sci.,* http://rjes.wdcb.ru

Pechersky, D. M. (2000), Global magnetic anomalies and the magnitudes of the secular variations of the geomagnetic field direction, *Geomagnetism and Aeronomy, 40,* 128–133.

Pechersky, D. M. (2001), The total magnitude of secular variations, global magnetic anomalies, and plumes, *Physics of the Earth,* (5), 85–91.

Pechersky, D. M., D. P. Naidin, and E. A. Molostovsky (1983), The Santonian-Campanian reversed polarity magnetozone and the Late Cretaceous magnetostratigraphical time-scale, *Cretaceous Res., 4*(3), 251–257.

Shcherbakov, V. P., G. M. Solodovnikov, and N. K. Sycheva (2002), Changes in the geomagnetic dipole value during the last 400 million years (volcanic rocks), *Physics of the Earth,* (2), 26–33.

Smith, J., and W. G. H. Z. ten Kate (1982), Trace-element patterns at the Cretaceous-Tertiary boundary: Consequences of a large impact, *Cretaceous Res., 2,* 307–322.

Tanaka, H., and M. Kono (1994), Paleointensity database provides new resource, *Eos Trans. AGU, 75,* 498.

Veimarn, A. B., D. P. Naidin, L. F. Kopaevich, A. S. Alekseev, and M. A. Nazarov (1998), *Global Catastrophic Events and Their Role in the Stratigraphic Correlations of Sedimentary Basins of Different Types,* 198 pp., Moscow State University, Moscow.

D. M. Pechersky, Institute of Physics of the Earth, Russian Academy of Sciences, 10 Bol'shaya Gruzinskaya ul., Moscow, 123995 Russia

A. V. Garbuzenko, Geological Institute, Russian Academy of Sciences, 7 Pyzhevskii per., Moscow, 109017 Russia

(Received 15 March 2005)